Oceanographic structure and seasonal variation contribute to high heterogeneity in mesozooplankton over small spatial scales

Manoela Brandão, Thierry Comtet, Patrick Pouline, Caroline Cailliau, Aline Blanchet-Aurigny, Marc Sourisseau, Raffaele Siano, Laurent Memery, Frédérique Viard, Flávia Nunes

Published in ICES J. Mar. Sci (2021) - https://doi.org/10.1093/icesjms/fsab127

Oceanographic structure and seasonal variation contribute to high heterogeneity in mesozooplankton over small spatial scales

Manoela C. Brandão[1*], Thierry Comtet[2], Patrick Pouline[3], Caroline Cailliau[3], Aline Blanchet-Aurigny[1], Marc Sourisseau[4], Raffaele Siano[4], Laurent Memery[5], Frédérique Viard[6], and Flavia Nunes[1*]

[1]Ifremer Centre de Bretagne, DYNECO, Laboratory of Coastal Benthic Ecology, Plouzané, France

[2]Sorbonne Université, CNRS, UMR 7144 AD2M, Station Biologique de Roscoff, Place G. Teissier, Roscoff, France

[3]Office Français de la Biodiversité, Parc Naturel Marin d'Iroise, Le Conquet, France

[4]Ifremer Centre de Bretagne, DYNECO, PELAGOS, Plouzané, France

[5]Laboratoire des Sciences de l'Environnement Marin (LEMAR), UMR CNRS/IFREMER/IRD/UBO 6539, Plouzané, France

[6]ISEM, Univ Montpellier, CNRS, EPHE, IRD, Montpellier, France

[*]Corresponding authors: manoela.costa.brandao@ifremer.fr (MCB), flavia.nunes@ifremer.fr (FN)

Abstract

The coastal oceans can be highly variable, especially near ocean fronts. The Ushant Front is the dominant oceanographic feature in the Iroise Sea (NE Atlantic) during summer, separating warm

stratified offshore waters from cool vertically-mixed nearshore waters. Mesozooplankton community structure was investigated over an annual cycle to examine relationships with oceanographic conditions. DNA metabarcoding of COI and 18S genes was used in communities from six sites along two cross-shelf transects. Taxonomic assignments of 380 and 296 OTUs (COI and 18S respectively) identified 21 classes across 13 phyla. Meroplankton relative abundances peaked in spring and summer, particularly for polychaete and decapod larvae respectively, corresponding to the reproductive periods of these taxa. Meroplankton was most affected by season, while holoplankton varied most by shelf position. Copepods with a mixed feeding strategy were associated with the most offshore sites, especially in the presence of the front, while filter-feeding or carnivorous copepods were associated with nearshore sites. In sum, mesozooplankton communities in well-mixed coastal waters were distinct from those found in the Ushant Front (high thermal stratification and chlorophyll-a). Furthermore, the benthic compartment, through its partial life cycle in the water column, contributed to high heterogeneity in planktonic communities over short temporal and spatial scales.

Keywords: Mesozooplankton, mitochondrial COI, 18S rRNA, DNA metabarcoding, High-throughput sequencing, Marine Protected Area, Ocean front

Introduction

The coastal oceans can be highly variable, influenced not only by major oceanographic regimes, but also by processes related to bordering landmasses, such as river discharge, runoff, tidal forcing and currents influenced by the coastline and shallow water columns. Nearshore conditions can therefore be highly contrasted to adjacent offshore water masses, with the most

striking examples being near ocean fronts. Ocean fronts occur where two distinct water masses come into contact, and are among the main oceanographic structures affecting the distribution of marine organisms as diverse as pelagic crustaceans, fish, marine mammals and birds (Acha *et al.*, 2015). They can arise from a diversity of processes and are defined by strong horizontal gradients of salinity and/or temperature. These hydrological structures create vertical fluxes, leading to aggregation processes, as well as increases in downward export or nutrient availability (Acha *et al.*, 2015). Ocean fronts have been shown to play an important role on plankton distribution, by aggregating, transporting, or separating specific assemblages (Marra *et al.*, 1990; Flint *et al.*, 2002; Ohman *et al.*, 2012). In particular, the fronts formed in the transition between coastal bays and their oceanic adjacent regions affect the distribution of meroplankton (i.e. mainly composed of pelagic larvae of invertebrates) (Shanks *et al.*, 2003; Ayata *et al.*, 2011; Brandão *et al.*, 2020). Consequently, fronts may play a role in the dispersal of species with a bentho-pelagic life cycle, potentially altering their broad-scale connectivity and distribution along the coasts (Acha *et al.*, 2015). Furthermore, because they affect ecosystem functions such as primary productivity, biogeochemical cycling and biomass production (Woodson and Litvin, 2015), ocean fronts also affect ecosystem services (Martinetto *et al.*, 2020), particularly fisheries. As such, the influence of ocean fronts on coastal communities merits adequate investigations.

The Iroise Sea, where the northeastern Atlantic transitions into the English Channel, constitutes an interesting environment for examining the effects of ocean fronts on pelagic communities. This part of the coast of western Brittany (France) is characterized by a megatidal regime (5 - 10 m tidal amplitudes), which generates strong tidal currents. Tidal friction produces enough turbulence to constantly mix the entire water column in nearshore areas, but as depth increases, tidal mixing is not sufficient to erode the seasonal thermocline (Brumer *et al.*, 2020).

The result is a tidally influenced thermal front called the Ushant Front that is characterized by a strong temperature gradient that separates warm stratified offshore waters from cool vertically mixed nearshore waters (Le Boyer *et al.*, 2009; Chevallier *et al.*, 2014; Cadier *et al.*, 2017a). Where nearshore and offshore water masses meet, a frontal zone is generated with specific characteristics between both water masses, such as thermal stratification coupled with high chlorophyll-a near the thermocline, which results from either subduction of productive coastal upper layers or nutrient enrichment due to mixing of the two water masses (or both). The Ushant Front is the dominant feature of the summer oceanographic structure of the Iroise Sea, which usually occurs from April/May to October every year (Chevallier *et al.*, 2014; Cadier *et al.*, 2017a). This front is known to increase primary production (Videau, 1987) but also to influence the size and abundance of phytoplankton (Pingree *et al.*, 1975; Landeira *et al.*, 2014), with longer diatom chains during the frontal establishment (Landeira *et al.*, 2014). This coastal front also acts as an ecological boundary for free-living bacteria, with photosynthetic bacteria being most abundant offshore of the front, oligotrophic bacteria being more abundant in water masses with low phytoplankton and high inorganic nutrients, and opportunistic copiotrophic bacteria being most abundant in the most productive period of the year, associated with the front (Lemonnier *et al.*, 2020). In addition, the mesozooplankton community showed its highest diversity at the front as a result of the co-occurrence of species from stratified and mixed waters (Schultes *et al.*, 2013).

The Ushant Front occurs within the boundaries of the Iroise Marine Natural Park (*Parc Naturel Marin d'Iroise*, PNMI), the oldest marine protected area (MPA) in France. Due to its influence on primary productivity and planktonic communities the front may affect the stocks of planktivorous fish, in particular sardines and anchovies, which are important fisheries in the Iroise

91 Sea. To better understand these potential effects, the PNMI has established a monitoring program
92 that has been in place for 10 years.
93 DNA metabarcoding, which combines high-throughput sequencing technologies with
94 DNA barcoding, is revolutionizing how biodiversity is assessed in the marine environment (Baird
95 and Hajibabaei, 2012; Cristescu, 2014), by allowing DNA taken from environmental (e.g. water,
96 sediment) or bulk (e.g. plankton) samples to be sequenced concurrently, followed by taxonomic
97 assignment by comparison to a reference sequence database, such as the Barcode of Life Data
98 Systems for COI (Ratnasingham and Hebert, 2007). Thus, species diversity can be recovered
99 across many broad taxonomic groups (Valentini *et al.*, 2016). In order to capture a representative
100 sample of community biodiversity, multiple loci are often used in metabarcoding due to their
101 complementarity, as there is a trade-off between the taxonomic resolution and the taxonomic range
102 recovered (Carroll *et al.*, 2019; Couton *et al.*, 2019). Metabarcoding has been broadly applied for
103 benthic monitoring of marine ecosystems (Fonseca *et al.*, 2010; Lejzerowicz *et al.*, 2015; Cowart
104 *et al.*, 2020), and a growing number of studies are now using DNA metabarcoding to examine
105 zooplankton community dynamics (Chain *et al.*, 2016; Stefanni *et al.*, 2018; Carroll *et al.*, 2019;
106 Couton *et al.*, 2019; Questel *et al.*, 2021). Although metabarcoding is considered semi-quantitative
107 due to methodological biases (Clarke *et al.*, 2017; Carroll *et al.*, 2019), other studies have recently
108 revealed significant positive correlations between total abundance counts from morphological
109 taxonomic identification and metabarcoding sequence numbers (Bucklin *et al.*, 2019; Schroeder
110 *et al.*, 2020), thus indicating that relative abundances of reads can be considered as a proxy of
111 relative abundances of taxa. Furthermore, metabarcoding applied to a time-series of meroplankton
112 showed variations in read abundances that corresponded well with expectations based on the
113 reproductive season of the identified species (Couton *et al.*, 2019). In addition, despite the potential

biases associated with metabarcoding, the method does present various advantages, such as the greater power for taxonomic identification for some groups, including undescribed or cryptic taxa, reducing time-consuming counts under the microscope, and the ability to recover information for a broad range of organisms (Lindeque *et al.*, 2013; Clarke *et al.*, 2017; Deagle *et al.*, 2018).

In this study, we investigated the composition of the mesozooplankton in the Iroise Sea and the potential role of an ocean front in shaping this community over the course of the year. We were particularly interested in the two contrasting groups of the mesozooplankton: meroplankton (partial life-cycle in the water column) and holoplankton (full life-cycle in the water column). Our specific goals were (i) to investigate the spatial and temporal distribution of mero- and holoplankton in the Iroise Sea using DNA metabarcoding of the mitochondrial COI and the nuclear ribosomal 18S genes, and (ii) to examine the environmental variables, including the ocean front characteristics, that best explain differences observed in the mero- and holoplankton community composition. Our central hypothesis is that the establishment of the Ushant Front in summer has an impact on the structure of the mesozooplankton community in the Iroise Sea, increasing its diversity.

Materials and Methods

Sample collection

Mesozooplankton sampling took place in the Iroise Marine Natural Park (*Parc Naturel Marin d'Iroise*, PNMI), a marine protected area (MPA) that covers 3,550 km^2 of the Iroise Sea. Sampling in the MPA was achieved on board the Valbelle (PM 509) and Augustine (PM 510) PNMI vessels, and was part of a regular monitoring program, the PNMIR, which started in 2010.

The PNMIR consists in sampling along two parallel cross-shelf transects, in front of the bays of Brest (seven stations) and Douarnenez (six stations). For the present study, zooplankton was sampled in six stations, three in each transect, in spring (23-05-2019), summer (11-07-2019) and fall (22-10-2019 to 24-10-2019) (Fig. 1a). Previous work has shown that the Ushant front usually occurs in summer and fall (June – September). In order to examine the potential effect of frontal conditions, sampling dates were chosen to capture conditions before, during and after the establishment of the Ushant Front. Vertical tows were performed from 5 m above the bottom to the surface with a WP2 plankton net with a 200-µm mesh size (UNESCO, 1968), equipped with a flowmeter (KC Denmark). Plankton was then sieved (200 µm) in order to remove seawater, and preserved onboard in a guanidinium thiocyanate buffer, not exceeding the volume of 100 ml.

To describe the abiotic conditions associated with each plankton sample, vertical profiles of temperature, salinity, fluorescence and turbidity were performed using a CTD probe (Seabird SBE19) coupled to a fluorimeter (NKE Mpx). Data from additional stations (four in the transect of Bay of Brest and three in the transect of Bay of Douarnenez; Fig. 1b-d) followed in the PNMIR monitoring program, taken on the same day of sampling, were included to better characterize the water column. An index of the thermal stratification (ΔT) was calculated as the difference between the surface and the bottom temperatures. A value higher than 1.5°C was considered as characterizing a stratified water column (Schultes *et al.*, 2013).

DNA extraction, PCR amplification and sequencing

DNA was preserved in a guanidine thiocyanate buffer which effectively lysed the plankton samples at room temperature over the course of one week, thereby eliminating the need for filtering samples post-collection. Two replicate DNA extractions were performed using 20 mL of each

plankton sample following homogenization by inversion, with a 2:1 volume of phenol:chloroform:isoamyl alcohol and 1:1 of an extraction buffer, followed by precipitation with 2:1 volume of isopropanol, 2 washes with 70% ethanol, resuspension in Milli-Q water and treatment with RNase A (10 mg/ml; Sigma-Aldrich, St. Louis, MO, USA) (Fukami *et al.*, 2004).

The primers mlCOIintF (5'-GGWACWGGWTGAACWGTWTAYCCYCC-3') (Leray *et al.*, 2013) and jgHCO2198 (5'-TAIACYTCIGGRTGICCRAARAAYCA-3') (Geller *et al.*, 2013) were used to amplify a 313-bp portion of the highly variable mitochondrial Cytochrome c Oxidase subunit I (COI) gene. In addition, the primers SSU_F04 (5'-GCTTGTCTCAAAGATTAAGCC-3') (Fonseca *et al.*, 2010) and SSU_R22mod (5'-CCTGCTGCCTTCCTTRGA-3') (Sinniger *et al.*, 2016) were used to amplify a ca. 450-bp portion of the V1–V2 regions of the nuclear small subunit rDNA (18S rDNA). Primers including Illumina sequencing adaptors are detailed in Table S1.

For each marker, four PCR reactions (20 µl final volume) were run for each of the two DNA extractions, for a total of eight PCRs per biological sample, containing 1µl of total DNA template, 1µl of each primer, 0.5µl of BSA (New England Biolabs), 6.5µl of ultrapure water, and 10µl of Q5 High-Fidelity 2X Master Mix (New England Biolabs). For COI, due to inosine content in the reverse primer, the Q5U Hot Start High-Fidelity DNA Polymerase (New England Biolabs) was used instead. Cycling conditions for COI started with a 2-min denaturation step followed by 16 initial cycles of 98°C for 10s, 30s at 62°C (-1°C per cycle), 72°C for 60s, followed by 25 cycles at 46°C annealing temperature, and a final extension of 72°C for 2 min (modified from Leray *et al.*, 2013). For 18S, cycling included a 2-min denaturation step followed by 30 cycles of 98°C for 10s, 30s at 57°C, 72°C for 30s, and a final extension of 72°C for 2 min (modified from Fonseca *et al.*, 2010). The positive amplifications were identified on a 1.5% agarose gel stained with GelRed (Biotium). PCR products from the eight replicates per biological sample were pooled at equal

183 volumes. Then a second PCR was done to add the Illumina index. These PCR products were
184 quantified using an Epoch spectrophotometer (BioTek Instruments) and pooled at equimolar
185 amounts. Paired-end reads (2 × 250 bp) were generated on a MiSeq (Illumina) at the Get-PlaGe
186 Genomics platform (Toulouse, France).
187
188 ## Read processing and taxonomic assignment
189 Resulting raw sequence reads were processed with the FROGS v.2.0 pipeline (Escudié *et*
190 *al.*, 2018), implemented on a Galaxy interface (Goecks *et al.*, 2010). First, paired-end reads were
191 merged into contigs with the FLASH algorithm (Magoč and Salzberg, 2011) before filtering by
192 length (minimum 250 bp for COI, and 350 bp for 18S). Chimera and singleton were filtered using
193 the VSEARCH tool (Rognes *et al.*, 2016) in each sample, and the remaining sequences underwent
194 SWARM v3.0 clustering, using the default parameters (Mahé *et al.*, 2014). SWARM uses a
195 clustering algorithm with a threshold corresponding to the maximum number of differences
196 between two sequences in an OTU (Mahé *et al.*, 2014).
197 Each representative OTU sequence was aligned and assigned to a taxon using BLAST,
198 with the following reference databases: BOLD_COI (https://www.boldsystems.org/) and Silva
199 18S rRNA v132 (https://www.arb-silva.de/) for COI and 18S, respectively. Potential false-positive
200 OTUs were removed by filtering OTUs representing less than 0.005% of the OTU reads (Bokulich
201 *et al.*, 2013).
202 In addition, we assigned trophic regime traits for the copepods, due to their high relative
203 abundance and important role in the pelagic community. Traits respective to trophic regime
204 (omnivore-herbivore, omnivore-detritivore, omnivore, carnivore), and feeding strategy (filter,

cruise, active ambush and mixed) were determined based on two available reference datasets (Benedetti *et al.*, 2015; Brun *et al.*, 2017).

Data analyses

Vertical profiles of environmental data (temperature, salinity and fluorescence) were generated using CTD cast data in Ocean Data View (Schlitzer, 2016). In addition, we used weekly averaged satellite images of sea surface temperatures (SST) for the sampling dates. Images were obtained from NASA MODIS Aqua Global Level 3 (NASA OBPG, 2020).

In order to account for differences in sequencing depth among samples, rarefaction to an equivalent number of reads (minimum of 59,000 and 56,000 reads for COI and 18S, respectively) was applied to all samples. Filtered rarefied data were used for Nonmetric Multidimensional Scaling (nMDS) ordination and hierarchical clustering, according to the community composition of mero- and holoplankton, which were sorted at the family level (Table S2). A resemblance matrix was generated using Euclidean distances based on Hellinger-transformed rarefied read abundances. Permutational multivariate analysis of variance (PERMANOVA) was conducted to test the statistical significance of groups formed *a priori* (factors shelf position and season), as well as of their interaction (Anderson, 2001).

In order to assess the relationship between the distribution of the main mesozooplankton groups and the environmental variables, a Redundancy Analysis (RDA) was conducted. In order to avoid collinearity of explanatory variables, we applied a variance inflation factor (VIF) and removed collinear variables. A cut-off VIF value of 10 (Zuur *et al.*, 2009) was applied to get the final set of covariates (distance from the coast, temperature, salinity, fluorescence, and thermal stratification), which excluded depth and turbidity. Mean values of temperature, salinity and

fluorescence of each vertical CTD profiles were used in the RDA analysis. Read abundances were transformed using the Hellinger transformation to reduce the wide disparity in magnitude of the number of reads between taxa (Legendre and Gallagher, 2001). Taxa that represented less than 5% of the reads were not included in this analysis.

In addition, we calculated the Shannon diversity index, considering OTUs as proxies of species, as used previously for estimating plankton diversity (e.g. Ibarbalz *et al.*, 2019).

The analyses were performed with the R v3.5.2 environment (R foundation Core Team, 2018). The normalization, RDA, nMDS, clustering, PERMANOVA and additional tests were conducted with the packages *vegan* (Oksanen *et al.*, 2008) and *HH* (Heiberger, 2020).

Results

Hydrological structure

Variations in temperature profiles between sampling dates were observed in the Iroise Sea (Fig.1b-d; Fig. S1). Surface temperature reached 18°C in both transects during summer (Fig.1c; Fig. S1b), while it did not exceed 15°C during spring and fall (Fig. 1b,d; Fig. S1a,c). The water column was well-mixed during spring and fall (Fig. 1b,d), while it was strongly stratified during summer in the offshore stations, in both transects, as shown by the stratification index (ΔT) (Fig. 1c). This showed that the westernmost stations (B7 and D6) were located in the frontal zone, where water masses come into contact and mix (Fig. 1b). To a lesser extent, the nearshore stations, especially the one located at the entrance of the bay of Douarnenez (D2), were also stratified (Fig. 1c).

Regarding fluorescence, values ranged between 0.5 and 15 µg l^{-1}, with highest values observed during spring and summer (Fig. S2). Peaks were observed below 5 m during spring, and at mid-depth (15-20 m) during summer for the Brest transect, especially at station B7 (Fig. S2a,b). Salinity increased offshore, especially during spring (Fig. S3). However, the range of values was very narrow (between 34.5 and 35.5) regardless of the sampling time or location.

Taxonomic composition

After bioinformatic filtering, the high-throughput sequencing effort yielded a total of 1,143,663 reads for the COI, and 1,039,947 for the 18S datasets. Additional information on number of reads before processing, as well as mean number of reads per sample can be found in Table S3.

From the 380 and 296 metazoan OTUs (for COI and 18S, respectively), 95% belonged to six phyla: Arthropoda (241 and 169 OTUs), Mollusca (47 and 33 OTUs), Cnidaria (31 and 40 OTUs), Annelida (19 and 12 OTUs), Chordata (12 and 14 OTUs), and Echinodermata (15 and 9 OTUs) (Table 1), with Arthropoda, especially copepods, representing nearly 60% of those. The remaining 5% belonged to seven phyla that contained no more than 14 OTUs each (COI and 18S combined) (Table 1).

Regarding the relative abundance (proportion of reads) over all samples combined, the mesozooplankton community was dominated by copepods (61.2%), hydrozoans (9.7%), appendicularians (8.5%), branchiopods (mainly cladocerans, 5.9%), chaetognaths (5.4%), ctenophores (3.4%), polychaetes (2.5%), and malacostracans (euphausiids, amphipods and decapods, 1.8%) (Table 1). The results obtained with both molecular markers were generally consistent. However, the spatial distribution of some groups, such as Chaetognatha in spring (Fig. 2a,d) or Malacostraca in summer (Fig. 2b,e), was quite different when estimated with COI or 18S.

In addition, Porifera and Ostracoda were only detected with COI, while Cnidaria and Appendicularia had lower relative abundances with COI (Fig. 2a-f).

Community structure varied over the course of the year, for instance, with polychaetes and chaetognaths being more representative in spring (Fig. 2a,d), and malacostracans, branchiopods and ctenophores in summer (Fig. 2b,e). During fall, the community composition was mainly homogeneous along the stations, largely dominated by copepods and appendicularians (Fig. 2i,l). The Shannon diversity index of the mesozooplankton community was slightly higher with COI as compared with 18S (Fig. 2a-f). Overall, a cross-shelf pattern was observed for diversity, with higher values closer to the coast and lower values in the most offshore stations (Fig. 2a-f). This trend did not vary over time.

Holoplankton dominated the mesozooplankton community in the Iroise Sea, whatever the transect and sampling time (Fig. 2g-l). Overall, meroplankton depicted an increase towards the coast, and were more abundant during summer.

Taking a closer look at the meroplankton community, the effect of sampling time was the most striking feature observed (Fig. 3a-c). This was exemplified by the near absence of reads assigned to Decapoda in spring and their large relative abundance in summer in both transects. This feature was statistically confirmed by the PERMANOVA that showed a significant effect of sampling time on the composition of meroplankton (Table 2), and was also observed in the nMDS and clustering analyses (Fig. 4a-b for COI; Fig. S4a-b for 18S). Conversely, no significant effect of the shelf position was observed on the taxonomic composition of meroplankton, meaning that the composition is stable across the shelf, at these high taxonomic levels (Table 2). Regarding the taxonomic composition, polychaete larvae were remarkably more abundant in spring (Fig. 3a). In turn, cnidarians (here exclusively hydroids), were mostly dominant in fall (Fig. 3c). Echinoderm

296 larvae were also found in greater numbers during fall (Fig. 3c), while decapod larvae were very
297 abundant during summer, and mainly in the most nearshore stations (Fig. 3b). Overall, the Shannon
298 index for meroplankton showed an increase towards the coast (Fig. 3a-c).

299 Meroplankton composition is shown at the family level for the most represented phylum
300 (Echinodermata), classes (Polychaeta and Bivalvia), and order (Decapoda) in Fig. 5. Overall, the
301 Shannon diversity index was higher towards the shore for most groups, with a few exceptions, in
302 accordance with the general trend observed for the whole meroplankton community (Fig. 3a-c). In
303 addition, Shannon indices were generally higher during spring and summer, and lower during fall.
304 Decapods were however one exception, presenting the highest diversity values during summer.
305 Generally, the meroplankton community showed a highly heterogeneous distribution over
306 relatively short spatial distances (stations were less than 30 km apart), as well as over time.
307 Substantial changes were also observed over seasons. For instance, amid echinoderms, larvae of
308 echinoids and holothurians were dominant during spring and summer, while larvae of ophiuroids
309 were mainly dominant during summer and fall (Fig. 5a-c). Polychaete larvae were dominated by
310 the families Oweniidae and Pectinariidae (Fig. 5d-f). Among bivalves, Mytilidae were dominant
311 during all three seasons, with contribution of Pectinidae during spring, and of Hiatellidae during
312 summer and fall (Fig. 5g-i). For decapods, caridean shrimps and brachyuran crabs were present
313 during all seasons, while anomuran crabs were only present during spring and summer, being
314 notably dominant during the warmest season (Fig. 5j-l).

315 In contrast to meroplankton, the Shannon diversity of holoplankton was relatively
316 homogeneous among months, but showed a decrease towards the nearshore stations (Fig. 3d-f).
317 The community was largely dominated by copepods, then by chaetognaths, appendicularians,
318 brachiopods and ctenophores. Pelagic polychaetes were also present in the community, mainly

during spring (Fig. 3d), while copepods were less represented in the offshore stations in spring and summer (Fig. 3d,e). Shelf position was a significant factor for the holopelagic community with both markers (Fig. 4c-d; Table 2; Fig. S4c-d). Season was also a significant factor for the holoplankton community, but only with the 18S marker (Table 2; Fig. S4c-d), probably due to more marked differences between months in comparison with the COI dataset. For instance, 18S revealed higher relative abundance of appendicularians in fall and of polychaetes in spring (Fig. 2d-f).

Regarding the holoplankton, 183 OTUs were assigned to copepods with COI, which belonged to 16 families (Fig. 6a-c). Shannon diversity values were relatively constant, showing however a decreasing trend towards the coast. Calanoids were largely dominant in the area during the sampling seasons, followed by cyclopoids. The calanoids Acartiidae, Temoridae and Paracalanidae were the most abundant overall (Fig. 6a-c). During fall, a higher number of families were present in the area, with the notable contribution of Centropagidae, Corycaeidae and Oncaeidae, in addition to the regularly dominant calanoids (Fig. 6c).

Regarding copepod feeding traits, most were filter feeders with an omnivore-herbivore trophic regime (Fig. 6d-i). Some spatial patterns were observed, with an increased proportion of copepods with a mixed feeding strategy towards the offshore stations (Fig. 6g,i). In addition, omnivore-detritivore copepods increased offshore during fall (Fig. 6f).

Mesozooplankton distribution in relation to the oceanographic structure

Regarding the influence of environmental variables on the distribution of the meroplankton, holoplankton and copepod feeding traits, the first and second axes of the Redundancy Analysis (RDA) ordination accounted together for 58.0%, 63.8, and 53.6% of the

342 constrained variance, respectively (Fig. 7; Table S4). All ordinations showed the segregation of
343 sampling times, with samples collected in summer being more distinct than those collected in
344 spring and fall (Fig. 7). This seems to be mainly driven by the unique thermohaline condition of
345 summer in the Iroise Sea, with a warmer and stratified water column, especially in the outer shelf
346 stations (yellow squares) (Fig. 7). Distance from the coast was an important factor, thus describing
347 the cross-shelf gradient, as clearly depicted along the ordinations (Fig. 7). Among meroplankton,
348 polychaete and mollusc larvae were mainly related to nearshore and intermediate shelf
349 environmental conditions, as opposed to cnidarians, which were found offshore (Fig. 7a). Amid
350 holoplankton, copepods showed an association with the nearshore stations (Fig. 7b). Regarding
351 the ordination for holoplanktonic groups, axis 2 mainly described the thermohaline gradient, with
352 highest temperature and thermal stratification (ΔT) opposed to salinity (Fig. 7b). Among the taxa,
353 brachiopods and ctenophores seemed to be the most associated with the summer conditions (Fig.
354 7b). For meroplankton, malacostracans (decapod larvae) were mostly associated with nearshore
355 summer stations (yellow circles) (Fig. 7a). Filter feeders and omnivore-herbivore copepods were
356 associated with summer warmer and stratified conditions (Fig. 7c).
357

358 Discussion

359 Here we investigated spatio-temporal variation in the composition of the mesozooplankton
360 community in a marine protected area (MPA) in the northeast Atlantic Ocean, based on a multi-
361 locus DNA metabarcoding approach.
362

363 Meroplankton contributes to mesozooplankton community structure across
364 seasons

The mesozooplankton community composition based on DNA metabarcoding data showed significant differences throughout the year, consistently with both markers. This is coherent with temporal variation described for temperate oceans, in response to oceanographic conditions (Thomas and Nielsen, 1994; Beaugrand *et al.*, 2010). The CTD profiles revealed a clear spring-to-summer transition in the Iroise Sea, represented by the stratification of the water column, and the establishment of the Ushant Front in July, with the most offshore stations (B7 and D6) being located in the frontal zone. Although our dataset did not include monthly sampling, inspection of satellite SST images showed that the front persisted in August and September 2019 (data not shown), while it was no longer present in October.

Mesozooplankton community structure was particularly strong in the meroplankton component over the course of the year, with abundant polychaete larvae during spring and decapod larvae during summer, for instance. In agreement with the present findings, and, importantly, using the same sampling gear (i.e. 200-µm WP2 net), a 20-year time-series from the Western English Channel (station L4), also reported a peak of polychaete larvae in late spring, of decapod larvae in June/July, and of echinoderm larvae in August and September (Highfield *et al.*, 2010). This time series also found that seasonal variation accounted for the main changes in the composition of the meroplankton, in addition to inter-annual variability. We hypothesize that the marked temporal variation found for meroplankton in the Iroise Sea was due to two main factors, the spawning/reproductive periods of species and the availability of food for the larvae.

Known spawning times for the most abundant bentho-pelagic species in the Iroise Sea coincided with peaks in meroplankton proportions in spring and summer. For instance, the polychaete *Lagis koreni* (Pectinariidae) is known to have its main spawning period from April to June (Nicolaidou, 1983) in agreement with our detection of a peak in polychaete larvae in spring.

388 Another study in the NE Atlantic, including the area off the bay of Douarnenez, also found larvae
389 of *L. koreni* in May and June (Ayata *et al.*, 2011). In addition, *Ophiothrix fragilis* and *Ophiocomina*
390 *nigra*, two co-occurring ophiuroids very abundant in the area (Blanchet-Aurigny *et al.*, 2012;
391 Guillam *et al.*, 2020), were detected in all sampling periods, particularly in fall. Both have extended
392 breeding seasons, with spawning taking place at approximately monthly intervals from April to
393 October (Smith, 1940), in agreement with our observations.
394 Changes in phytoplankton community structure may reflect differential bloom timings and
395 intensities, with high contributions of diatoms over dinoflagellates in spring and summer, observed
396 in previous reports in this region (Birrien *et al.*, 1991; Ragueneau *et al.*, 1994; Cadier *et al.*, 2017a).
397 In the Iroise Sea, spring blooms are associated with higher proportions of diatoms, followed by
398 moderate drops in diatom abundances in summer, with dinoflagellates being more preponderant
399 in fall (Cadier *et al.*, 2017a; Benedetti *et al.*, 2019). Diatom blooms are triggered by the seasonal
400 stratification in April-May, which creates favorable conditions in nutrients and irradiance allowing
401 large opportunistic diatoms to grow (Cadier *et al.*, 2017a). Phytoplankton continue to show high
402 concentrations throughout summer due to the replenishment of nutrients in the coastal waters
403 through the establishment of the Ushant Front (Cadier *et al.*, 2017a). The front may therefore favor
404 larval survival by increasing resources available in the zone of the front as compared to nearshore
405 waters (Cadier *et al.*, 2017a, 2017b).
406
407 Like meroplankton, copepods also showed strong temporal variations. Regarding family
408 compositions, Acartiidae were dominant in spring, while Temoridae and Paracalanidae were
409 present during all seasons. During fall, a higher number of copepod families were present. When
410 evaluating the temporal variability of mesozooplankton in the area, Benedetti *et al.* (2019) also

found higher contributions of Acartiidae in spring and a higher number of unidentified Calanoida in fall. With respect to the feeding traits, we observed the dominance of omnivore-herbivore filter-feeders overall, with an increase of omnivore-detritivores and carnivores in fall. In the North Atlantic, peaks of copepods that graze on phytoplankton have been seen in spring, while copepods that feed on microzooplankton and detritus were dominant in other seasons (Friedland *et al.*, 2016). Overall, omnivorous filter-feeding taxa (i.e. Temoridae and Paracalanidae copepods, appendicularians and cladocerans) represented the dominant trophic trait over the mesozooplankton community throughout the water column. To a lesser degree, carnivory was also an important feeding behavior, with Corycaeidae copepods peaking during fall, and hydrozoans and chaetognaths constituting the second and third most abundant groups in the area.

High spatial heterogeneity in the mesozooplankton community from the nearshore to offshore

Stratification of the water column and temperature were key factors in determining mesozooplankton community structure together with distance from the coast, reflecting the nearshore-offshore gradient, as these explain most of the variation of the first RDA components. In a previous study, using a nearshore-offshore transect in September 2009, Schultes *et al.* (2013) found that the East-West gradient was the main pattern of zooplankton abundance variations in the Iroise Sea. In our study, a noticeable differentiation along the cross-shelf gradient was observed, mainly in terms of community composition for holoplankton and Shannon diversity index for meroplankton. The inner stations had the highest level of diversity for meroplankton. This likely reflects the influence of larval export from the bays, which hosts abundant and highly diverse benthic communities (Chauvaud *et al.*, 2000; Gallon *et al.*, 2017). In addition, groups that are

434 known for their coastal affiliations (e.g. malacostracans and echinoderms) were associated with
435 nearshore and intermediate shelf environmental conditions.

436 Furthermore, we found that the mesozooplankton community was highly heterogeneous at
437 a small spatial scale, especially along the cross-shelf gradient. Changes in zooplankton community
438 composition between relatively nearby sites have been observed elsewhere, mainly attributed to
439 plankton patchiness and the presence of ocean fronts (Seda and Devetter, 2000; Trudnowska *et al.*,
440 2016). Plankton distribution and its patchiness are regulated by both biological and physical
441 processes that govern its abundance and community composition (Mackas *et al.*, 1985; Acha et
442 *al.*, 2015). In addition, the outflows from each of the bays may also play a role in the community
443 observed in the adjacent sampled area. The mixing intensity from the bays to the front leads to
444 localized and variable small oceanographic processes, contributing to the spatial variability even
445 within the coastal zone for the meroplankton community.

446 Mesozooplankton in the Iroise Sea provides a wide range of food resources for the higher
447 trophic levels. For example, crustaceans (small copepods, and decapod and cirriped larvae) are a
448 significant part of the diet of the sardine species *Sardina pilchardus*, a locally important
449 commercial species (Garrido *et al.*, 2008). Crustaceans are also an important food resource for the
450 exclusively planktivorous basking shark (*Cetorhinus maximus*), which annual sightings in the
451 Iroise Sea are associated with the Ushant Front (Sims, 2008), and for seabirds (Springer *et al.*,
452 2007). In addition, recent evidence showed that gelatinous zooplankton (ctenophores,
453 hydromedusae, chaetognaths and salps), which were also very abundant in our samples, form an
454 important part of fish diet with higher levels of protein, carbon content and other nutrients than
455 previously thought (Henschke *et al.*, 2016; Diaz Briz *et al.*, 2017).

Safeguarding the biodiversity of coastal waters and managing the sustainable exploitation of marine resources are the main objectives within the establishment of the Iroise Marine Natural Park. The plankton monitoring program (PNMIR) aims particularly to evaluate the interannual variations in the phyto- and zooplankton communities and their link with fisheries of commercially important species in the area, such as the European sardine *S. pilchardus* (Benedetti *et al.*, 2019). Regarding the influence of the Ushant Front in the pelagic communities, a longer monitoring time-series, with more frequent sampling would aid to follow the full cycle of the front. One further limitation of our observations is the absence of sampling in fully oligotrophic waters, offshore of the frontal zone. Sampling offshore would have allowed us to determine whether communities in the frontal zone represented a combination of nearshore and offshore taxa, or whether taxa specific to the frontal zone were present, as observed for phytoplankton (Landeira *et al.*, 2014). Offshore sampling was logistically difficult to implement with the resources available to the MPA, but future sampling and monitoring efforts that include sites beyond the frontal zone may improve our understanding of the dynamics of planktonic communities and their effects on trophic webs and biogeochemical cycles in the area. In addition, we recommend incorporating multi-marker DNA metabarcoding as a standard tool for biodiversity assessment and environmental monitoring time-series, as multiple compartments of the planktonic community sampled concurrently can be examined in parallel.

Conclusions

Our study is the first to implement DNA metabarcoding to document the spatial and temporal variations in the community composition and diversity of mesozooplankton in the Iroise Sea. Metabarcoding of mixed tissue samples allowed us to detect a diverse array of marine

zooplankton and examine changes in community structure across several different phyla. Although the mesozooplankton community was overwhelmingly dominated by holoplankton in terms of relative abundance of reads, meroplankton showed a relatively high contribution of taxa present in the area, expressed by the number of OTUs. It is worth pointing out that some meroplanktonic groups may be underestimated due to the size of the mesh (200 μm), notably bivalve larvae.

Our findings indicate that spring and summer are the periods with higher relative abundances and diversity for most meroplankton groups in the Iroise Sea, associated with the spawning period of benthic species and with favorable environmental conditions for the development of larvae, probably due to the presence of the Ushant Front. During fall, despite the presence of some meroplanktonic groups, holoplankton taxa dominate the mesozooplankton community in terms of relative abundance. Most meroplankters have likely settled by this time period, or less larvae are released, and that the holoplankton taxa present feed mainly on sinking and suspended particles (detritivores) and/or microzooplankton (carnivorous).

Our results for copepod feeding traits are in general agreement with observations for bacterial communities associated with the Ushant Front. Copiotrophic bacteria that recycle detrital organic matter were also dominant in communities following the period of the phytoplankton blooms (Lemonnier *et al.*, 2020). Both copepod and bacterial communities therefore appear to respond to increases in available organic matter post-bloom.

The significant small-scale spatial variation observed also reflect the strong nearshore-offshore gradient. In addition, the importance of the stratification of the water column reflects the influence of the Ushant Front in structuring the mesozooplankton community.In the future, the present findings should be integrated with the characterization of other target communities, such as

phytoplankton, bacterioplankton, prokaryotes and higher trophic levels, in order to present a full picture of the influence of the Ushant Front in the pelagic component of the Iroise Sea.

Acknowledgements

We thank Yannis Turpin, Rémy Destabeau, Arthur Hebert, Pierre Joffredo, Anne-Louise Blier, and Nathalie Dridi-Moreul for their help in sampling. We thank Louis Marié for providing the SST maps. We also thank Gabin Droual and Martin Marzloff for suggestions on data analyses and interpretation. This work was supported by the ISblue project, Interdisciplinary Graduate School for the Blue Planet (ANR-17-EURE-0015), co-funded by a grant from the French government under the program "Investissements d'Avenir", and by a grant from the Regional Council of Brittany (SAD programme). It was also supported by a grant from Ifremer (Politique de Site: LADIDA, to F. Nunes and T. Comtet). Sampling was conducted with support from the Iroise Marine Natural Park (*Parc Naturel Marin d'Iroise*), which is part of the *Office Français de la Biodiversité* (OFB). This is publication ISEM XX-XXX.

Data Availability Statement

The data will be made available within a DOI once the acceptance of the manuscript.

References

Acha, E.M., Piola, A., Iribarne, O. and Mianzan, E. 2015. Ecological Processes at Marine Fronts: Oases in the Ocean. Springer, Cham (68 pp).

Anderson, M. J. 2001. A new method for non-parametric multivariate analysis of variance. Austral Ecology, 26: 32–46.

Ayata, S. D., Stolba, R., Comtet, T., and Thiébaut, É. 2011. Meroplankton distribution and its relationship to coastal mesoscale hydrological structure in the northern Bay of Biscay (NE Atlantic). Journal of Plankton Research, 33: 1193–1211.

Baird, D. J., and Hajibabaei, M. 2012. Biomonitoring 2.0: A new paradigm in ecosystem assessment made possible by next-generation DNA sequencing. Molecular Ecology, 21: 2039–2044.

Beaugrand, G., Edwards, M., and Legendre, L. 2010. Marine biodiversity, ecosystem functioning, and carbon cycles. Proceedings of the National Academy of Sciences of the United States of America, 107: 10120–10124.

Benedetti, F., Gasparini, S., and Ayata, S. D. 2015. Identifying copepod functional groups from species functional traits. Journal of Plankton Research, 38: 159–166.

Benedetti, F., Jalabert, L., Sourisseau, M., Becker, B., Cailliau, C., Desnos, C., Elineau, A., *et al.* 2019. The seasonal and inter-annual fluctuations of plankton abundance and community structure in a North Atlantic Marine Protected Area. Frontiers in Marine Science, 6: 1–16.

Birrien, J. L., Wafar, M. V. M., Corre, P. Le, and Riso, R. 1991. Nutrients and primary production in a shallow stratified ecosystem in the Iroise Sea. Journal of Plankton Research, 13: 721–742.

Blanchet-Aurigny, A., Dubois, S. F., Hily, C., Rochette, S., Le Goaster, E., and Guillou, M. 2012. Multi-decadal changes in two co-occurring ophiuroid populations. Marine Ecology Progress Series, 460: 79–90.

Bokulich, N. A., Subramanian, S., Faith, J. J., Gevers, D., Gordon, J. I., Knight, R., Mills, D. A., *et al.* 2013. Quality-filtering vastly improves diversity estimates from Illumina amplicon sequencing. Nature Methods, 10: 57–59.

Brandão, M. C., Garcia, C. A. E., and Freire, A. S. 2020. Meroplankton community structure across oceanographic fronts along the South Brazil Shelf. Journal of Marine Systems, 208.

Brumer, S. E., Garnier, V., Redelsperger, J. L., Bouin, M. N., Ardhuin, F., and Accensi, M. 2020. Impacts of surface gravity waves on a tidal front: A coupled model perspective. Ocean Modelling, 154: 101677. Elsevier Ltd. https://doi.org/10.1016/j.ocemod.2020.101677.

Brun, P., Payne, M. R., and Kiørboe, T. 2017. A trait database for marine copepods. Earth System Science Data, 9: 99–113.

Bucklin, A., Yeh, H. D., Questel, J. M., Richardson, D. E., Reese, B., Copley, N. J., and Wiebe, P. H. 2019. Time-series metabarcoding analysis of zooplankton diversity of the NW Atlantic continental shelf. ICES Journal of Marine Science, 76: 1162–1176.

Cadier, M., Sourisseau, M., Gorgues, T., Edwards, C. A., and Memery, L. 2017a. Assessing spatial and temporal variability of phytoplankton communities' composition in the Iroise Sea ecosystem (Brittany, France): A 3D modeling approach: Part 2: Linking summer mesoscale distribution of phenotypic diversity to hydrodynamism. Journal of Marine Systems, 169: 111–126.

Cadier, M., Gorgues, T., Sourisseau, M., Edwards, C. A., Aumont, O., Marïï¿½, L., and Memery, L. 2017b. Assessing spatial and temporal variability of phytoplankton communities' composition in the Iroise Sea ecosystem (Brittany, France): A 3D modeling approach. Part 1: Biophysical control over plankton functional types succession and distribution. Journal of Marine Systems, 165: 47–68. The Authors. http://dx.doi.org/10.1016/j.jmarsys.2016.09.009.

Carroll, E. L., Gallego, R., Sewell, M. A., Zeldis, J., Ranjard, L., Ross, H. A., Tooman, L. K., *et al.* 2019. Multi-locus DNA metabarcoding of zooplankton communities and scat reveal trophic interactions of a generalist predator. Scientific Reports, 9: 1–14.

Chain, F. J. J., Brown, E. A., Macisaac, H. J., and Cristescu, M. E. 2016. Metabarcoding reveals strong spatial structure and temporal turnover of zooplankton communities among marine and freshwater ports. Diversity and Distributions, 22: 493–504.

Chauvaud, L., Jean, F., Ragueneau, O., and Thouzeau, G. 2000. Long-term variation of the Bay of Brest ecosystem: Benthic-pelagic coupling revisited. Marine Ecology Progress Series, 200: 35–48.

Chevallier, C., Herbette, S., Marié, L., Le Borgne, P., Marsouin, A., Péré, S., Levier, B., *et al.* 2014. Observations of the Ushant front displacements with MSG/SEVIRI derived sea surface temperature data. Remote Sensing of Environment, 146: 3–10. Elsevier Inc. http://dx.doi.org/10.1016/j.rse.2013.07.038.

Clarke, L. J., Beard, J. M., Swadling, K. M., and Deagle, B. E. 2017. Effect of marker choice and thermal cycling protocol on zooplankton DNA metabarcoding studies. Ecology and Evolution, 7: 873–883.

Couton, M., Comtet, T., Le Cam, S., Corre, E., and Viard, F. 2019. Metabarcoding on planktonic larval stages: An efficient approach for detecting and investigating life cycle dynamics of benthic aliens. Management of Biological Invasions, 10: 657–689.

Cowart, D. A., Matabos, M., Brandt, M. I., Marticorena, J., and Sarrazin, J. 2020. Exploring Environmental DNA (eDNA) to Assess Biodiversity of Hard Substratum Faunal Communities on the Lucky Strike Vent Field (Mid-Atlantic Ridge) and Investigate Recolonization Dynamics After an Induced Disturbance. Frontiers in Marine Science, 6: 1–21.

Cristescu, M. E. 2014. From barcoding single individuals to metabarcoding biological communities: Towards an integrative approach to the study of global biodiversity. Trends in Ecology and Evolution, 29: 566–571. Elsevier Ltd. http://dx.doi.org/10.1016/j.tree.2014.08.001.

585 Deagle, B. E., Clarke, L. J., Kitchener, J. A., Polanowski, A. M., and Davidson, A. T. 2018. Genetic monitoring of
586 open ocean biodiversity: An evaluation of DNA metabarcoding for processing continuous plankton recorder
587 samples. Molecular Ecology Resources, 18: 391–406.
588 Diaz Briz, L., Sánchez, F., Marí, N., Mianzan, H., and Genzano, G. 2017. Gelatinous zooplankton (ctenophores,
589 salps and medusae): an important food resource of fishes in the temperate SW Atlantic Ocean. Marine Biology
590 Research, 13: 630–644.
591 Escudié, F., Auer, L., Bernard, M., Mariadassou, M., Cauquil, L., Vidal, K., Maman, S., *et al.* 2018. FROGS: Find,
592 Rapidly, OTUs with Galaxy Solution. Bioinformatics, 34: 1287–1294.
593 Flint, M. V., Sukhanova, I. N., Kopylov, A. I., Poyarkov, S. G., and Whitledge, T. E. 2002. Plankton distribution
594 associated with frontal zones in the vicinity of the Pribilof Islands. Deep-Sea Research Part II: Topical Studies
595 in Oceanography, 49: 6069–6093.
596 Fonseca, V. G., Carvalho, G. R., Sung, W., Johnson, H. F., Power, D. M., Neill, S. P., Packer, M., *et al.* 2010.
597 Second-generation environmental sequencing unmasks marine metazoan biodiversity. Nature
598 Communications, 1: 1–8. Nature Publishing Group. http://dx.doi.org/10.1038/ncomms1095.
599 Friedland, K. D., Record, N. R., Asch, R. G., Kristiansen, T., Saba, V. S., Drinkwater, K. F., Henson, S., *et al.* 2016.
600 Seasonal phytoplankton blooms in the North Atlantic linked to the overwintering strategies of copepods.
601 Elementa, 2016: 1–19.
602 Fukami, H., Budd, A. F., Levitan, D. R., Jara, J., Kersanach, R., and Knowlton, N. 2004. Geographic differences in
603 species boundaries among members of the Montastraea annularis complex based on molecular and
604 morphological markers. Evolution, 58: 324–337.
605 Gallon, R. K., Lavesque, N., Grall, J., Labrune, C., Gremare, A., Bachelet, G., Blanchet, H., *et al.* 2017. Regional
606 and latitudinal patterns of soft-bottom macrobenthic invertebrates along French coasts: Results from the
607 RESOMAR database. Journal of Sea Research, 130: 96–106.
608 Garrido, S., Ben-Hamadou, R., Oliveira, P. B., Cunha, M. E., Chícharo, M. A., and Van Der Lingen, C. D. 2008.
609 Diet and feeding intensity of sardine Sardina pilchardus: Correlation with satellite-derived chlorophyll data.
610 Marine Ecology Progress Series, 354: 245–256.
611 Geller, J., Meyer, C., Parker, M., and Hawk, H. 2013. Redesign of PCR primers for mitochondrial cytochrome c
612 oxidase subunit I for marine invertebrates and application in all-taxa biotic surveys. Molecular Ecology
613 Resources, 13: 851–861.
614 Goecks, J., Nekrutenko, A., Taylor, J., Afgan, E., Ananda, G., Baker, D., Blankenberg, D., *et al.* 2010. Galaxy: a
615 comprehensive approach for supporting accessible, reproducible, and transparent computational research in
616 the life sciences. Genome Biology, 11.
617 Guillam, M., Bessin, C., Blanchet-Aurigny, A., Cugier, P., Nicolle, A., Thiébaut, É., and Comtet, T. 2020. Vertical
618 distribution of brittle star larvae in two contrasting coastal embayments: implications for larval transport.
619 Scientific Reports, 10. Nature Publishing Group UK. https://doi.org/10.1038/s41598-020-68750-4.
620 Heiberger, M. R. M. 2020. Package ‘ HH ’.
621 Henschke, N., Everett, J. D., Richardson, A. J., and Suthers, I. M. 2016. Rethinking the Role of Salps in the Ocean.
622 Trends in Ecology and Evolution, 31: 720–733. Elsevier Ltd. http://dx.doi.org/10.1016/j.tree.2016.06.007.
623 Highfield, J. M., Eloire, D., Conway, D. V. P., Lindeque, P. K., Attrill, M. J., and Somerfield, P. J. 2010. Seasonal
624 dynamics of meroplankton assemblages at station L4. Journal of Plankton Research, 32: 681–691.
625 Ibarbalz, F. M., Henry, N., Brandão, M. C., Martini, S., Busseni, G., Byrne, H., Coelho, L. P., *et al.* 2019. Global
626 Trends in Marine Plankton Diversity across Kingdoms of Life. Cell, 179.
627 Landeira, J. M., Ferron, B., Lunven, M., Morin, P., Marie, L., and Sourisseau, M. 2014. Biophysical interactions
628 control the size and abundance of large phytoplankton chains at the ushant tidal front. PLoS ONE, 9.
629 Le Boyer, A., Cambon, G., Daniault, N., Herbette, S., Le Cann, B., Marié, L., and Morin, P. 2009. Observations of
630 the Ushant tidal front in September 2007. Continental Shelf Research, 29: 1026–1037.
631 Legendre, P., and Gallagher, E. D. 2001. Ecologically meaningful transformations for ordination of species data.
632 Oecologia, 129: 271–280.
633 Lejzerowicz, F., Esling, P., Pillet, L. L., Wilding, T. a., Black, K. D., and Pawlowski, J. 2015. High-throughput
634 sequencing and morphology perform equally well for benthic monitoring of marine ecosystems. Scientific
635 Reports, 5: 13932. Nature Publishing Group. http://www.nature.com/doifinder/10.1038/srep13932.
636 Lemonnier, C., Perennou, M., Eveillard, D., Fernandez-Guerra, A., Leynaert, A., Marié, L., Morrison, H. G., *et al.*
637 2020. Linking Spatial and Temporal Dynamic of Bacterioplankton Communities With Ecological Strategies
638 Across a Coastal Frontal Area. Frontiers in Marine Science, 7: 1–13.
639 Leray, M., Yang, J. Y., Meyer, C. P., Mills, S. C., Agudelo, N., Ranwez, V., Boehm, J. T., *et al.* 2013. A new
640 versatile primer set targeting a short fragment of the mitochondrial COI region for metabarcoding metazoan

diversity: Application for characterizing coral reef fish gut contents. Frontiers in Zoology, 10: 1–14.
Lindeque, P. K., Parry, H. E., Harmer, R. A., Somerfield, P. J., and Atkinson, A. 2013. Next generation sequencing reveals the hidden diversity of zooplankton assemblages. PLoS ONE, 8: 1–14.
Mackas, D. L., Denman, K. L., and Abbott, M. R. 1985. Plankton patchiness: biology in the physical vernacular. Bulletin of Marine Science, 37: 653–674.
Magoč, T., and Salzberg, S. L. 2011. FLASH: Fast length adjustment of short reads to improve genome assemblies. Bioinformatics, 27: 2957–2963.
Mahé, F., Rognes, T., Quince, C., de Vargas, C., and Dunthorn, M. 2014. Swarm: Robust and fast clustering method for amplicon-based studies. PeerJ, 2014: 1–13.
Marra, J., Houghton, R. W., and Garside, C. 1990. Phytoplankton growth at the shelf-break front in the Middle Atlantic Bight. Journal of Marine Research, 48: 851–868.
Martinetto, P., Alemany, D., Botto, F., Mastrángelo, M., Falabella, V., Acha, E. M., Antón, G., *et al.* 2020. Linking the scientific knowledge on marine frontal systems with ecosystem services. Ambio, 49: 541–556.
NASA Ocean Biology Processing Group. 2020. Moderate-resolution Imaging Spectroradiometer (MODIS) Aqua SST Data; NASA OB.DAAC, Greenbelt, MD, USA. Accessed on 01/14/2021.
Nicolaidou, A. 1983. Life history and productivity of *Pectinaria koreni* Malmgren (polychaeta). Estuarine, Coastal and Shelf Science, 17: 31–43.
Ohman, M. D., Powell, J. R., Picheral, M., and Jensen, D. W. 2012. Mesozooplankton and particulate matter responses to a deep-water frontal system in the southern California Current System. Journal of Plankton Research, 34: 815–827.
Oksanen, J., Kindt, R., Legendre, P., O'Hara, B., Simpson, G. L., Solymos, P. M., Stevens, M. H. H., *et al.* 2008. The vegan package. Community ecology package: 190. https://bcrc.bio.umass.edu/biometry/images/8/85/Vegan.pdf.
Pingree, R. D., Pugh, P. R., Holligan, P. M., and Forster. 1975. Summer phytoplankton blooms and red tides along tidal fronts in the approaches to the English Channel. Nature, 258: 672–677.
Questel, J. M., Hopcroft, R. R., DeHart, H. M., Smoot, C. A., Kosobokova, K. N., Bucklin, A. 2021. Metabarcoding of zooplankton diversity within the Chukchi Borderland, Arctic Ocean: improved resolution from multi-gene markers and region-specific DNA databases. Marine Biodiversity, 51: 4.
R Core Team. 2018. R: A Language and Environment for Statistical Computing. R Foundation for Statistical Computing, Vienna, Austria, https://www.R-project.org/.
Ragueneau, O., Varela, E. D., Treguer, P., Queguiner, B., and Delamo, Y. 1994. Phytoplankton dynamics in relation to the biogeochemical cycle of silicon in a coastal ecosystem of Western Europe. Marine Ecology Progress Series, 106: 157–172.
Ratnasingham, S., and Hebert, P. D. N. 2007. The Barcode of Life Data System. Molecular Ecology Notes, 7: 355–364.
Rognes, T., Flouri, T., Nichols, B., Quince, C., and Mahé, F. 2016. VSEARCH: A versatile open source tool for metagenomics. PeerJ, 2016: 1–22.
https://doi.org/10.1016/j.pocean.2019.102202.
Schlitzer. 2016. Ocean Data View User's Guide Acknowledgements: 1–173. https://odv.awi.de/fileadmin/user_upload/odv/misc/odv4Guide.pdf.
Schroeder, A., Stanković, D., Pallavicini, A., Gionechetti, F., Pansera, M., and Camatti, E. 2020. DNA metabarcoding and morphological analysis - Assessment of zooplankton biodiversity in transitional waters. Marine Environmental Research, 160.
Schultes, S., Sourisseau, M., Le Masson, E., Lunven, M., and Marié, L. 2013. Influence of physical forcing on mesozooplankton communities at the Ushant tidal front. Journal of Marine Systems, 109–110: S191–S202. Elsevier B.V. http://dx.doi.org/10.1016/j.jmarsys.2011.11.025.
Seda, J., and Devetter, M. 2000. Zooplankton community structure along a trophic gradient in a canyon-shaped dam reservoir. Journal of Plankton Research, 22: 1829–1840.
Shanks, A. L., McCulloch, A., and Miller, J. 2003. Topographically generated fronts, very nearshore oceanography and the distribution of larval invertebrates and holoplankters. Journal of Plankton Research, 25: 1251–1277.
Sims, D. W. 2008. Chapter 3 Sieving a Living. A Review of the Biology, Ecology and Conservation Status of the Plankton-Feeding Basking Shark Cetorhinus Maximus. Advances in Marine Biology, 54: 171–220.
Sinniger, F., Pawlowski, J., Harii, S., Gooday, A. J., Yamamoto, H., Chevaldonné, P., Cedhagen, T., *et al.* 2016. Worldwide analysis of sedimentary DNA reveals major gaps in taxonomic knowledge of deep-sea benthos. Frontiers in Marine Science, 3: 1–14.
Smith, J. B. 1940. Memoirs: The Reproductive System and Associated Organs of the Brittle-Star Ophiothrix

Fragilis. Journal of Cell Science, s2-82: 267–309.
Springer, A. M., Byrd, G. V., and Iverson, S. J. 2007. Hot oceanography: Planktivorous seabirds reveal ecosystem responses to warming of the Bering Sea. Marine Ecology Progress Series, 352: 289–297.
Stefanni, S., Stanković, D., Borme, D., de Olazabal, A., Juretić, T., Pallavicini, A., and Tirelli, V. 2018. Multi-marker metabarcoding approach to study mesozooplankton at basin scale. Scientific Reports, 8: 1–13.
Thomas, K., and Nielsen, T. G. 1994. Regulation of zooplankton biomass and production in a temperate, coastal ecosystem. 1. Copepods. Limnology and Oceanography, 39: 493–507.
Trudnowska, E., Gluchowska, M., Beszczynska-Möller, A., Blachowiak-Samolyk, K., and Kwasniewski, S. 2016. Plankton patchiness in the Polar Front region of the west Spitsbergen Shelf. Marine Ecology Progress Series, 560: 1–18.
UNESCO. 1968. Monographs on Oceanographic Methodology: Zooplankton Sampling. UNESCO, Paris (174 pp).
Valentini, Taberlet P, Miaud C, Civade R, Herder J, Thomsen PF, Bellemain E, *et al.* 2016. Next-generation monitoring of aquatic biodiversity using environmental {DNA} metabarcoding. Molecular Ecology, 25: 929–942.
Videau, C. 1987. Primary production and physiological state of phytoplankton at the Ushant tidal front (west coast of Brittany, France). Marine Ecology Progress Series, 35: 141–151.
Woodson, C. B., and Litvin, S. Y. 2015. Ocean fronts drive marine fishery production and biogeochemical cycling. Proceedings of the National Academy of Sciences of the United States of America, 112: 1710–1715.
Zuur, A. F., Ieno, E. N., Walker, N. J., Saveliev, A. A., Smith, G. 2009. Mixed Effects Models and Extensions in Ecology with R. Springer, New York (574 pp).

Tables and Figures

Table 1. Number of reads and OTUs by Phylum and Class. Number of reads and OTUs assigned to Phylum and Class for COI and 18S markers, ordered by higher to lower number of reads.

			OTUs		Reads	
Phylum	**Class**	**Common name**	**COI**	**18S**	**COI**	**18S**
Arthropoda	Hexanauplia	copepods and barnacles	183	129	732,753	604,461
Cnidaria	Hydrozoa	jellyfish-like	31	39	86,787	124,656
Chordata	Appendicularia	tunicates	8	11	81,126	103,611
Arthropoda	Branchiopoda	planktonic crustaceans	13	8	50,340	79,308
Chaetognatha	Sagittoidea	arrow worms	6	7	61,803	56,037
Ctenophora	Tentaculata	comb jellies	8	6	64,110	10,926
Annelida	Polychaeta	polychaetes	19	12	25,458	28,851
Arthropoda	Malacostraca	crustaceans	41	32	22,356	16,944
Mollusca	Bivalvia	bivalves	33	21	8,757	7,788
Mollusca	Gastropoda	sea snails	14	12	2,655	1,926
Chordata	Actinopterygii	ray-finned fish	3	2	1,233	2,766
Chordata	Thaliacea	salps	1	1	1,269	1,875
Porifera	Demospongiae	sponges	1	-	3,075	-
Echinodermata	Ophiuroidea	brittle stars	6	4	771	426
Echinodermata	Echinoidea	sea urchins	6	4	411	117
Arthropoda	Ostracoda	ostracods	4	-	501	-
Echinodermata	Holothuroidea	sea cucumbers	3	1	258	171
Platyhelminthes	Rhabditophora	flatworm	-	1	-	27
Cnidaria	Anthozoa	jellyfish-like	-	1	-	18
Bryozoa	Gymnolaemata	moss animals	-	1	-	15

Phoronida		horseshoe worm	-	2	-	12
Nemertea	Palaeonemertea	marine worm	-	2	-	12
Metazoans			380	296	1,143,663	1,039,947

Table 2. Results of PERMANOVA. Results of the PERMANOVA comparing the mero- and holoplankton community composition between seasons and/or among shelf position, for COI and 18S genes.

COI				**18S**			
	df	**F**	***p***		**df**	**F**	***p***
Meroplankton				Meroplankton			
Season	2	1.89	0.011 *	Season	2	4.93	0.000 ***
Shelf position	2	0.67	0.907	Shelf position	2	1.98	0.298
S x SP	4	0.82	0.742	S x SP	4	1.16	0.460
Residual	9			Residual	9		
Holoplankton				Holoplankton			
Season	2	1.99	0.054	Season	2	3.45	0.000 ***
Shelf position	2	4.03	0.005 **	Shelf position	2	4.32	0.000 ***
S x SP	4	1.12	0.709	S x SP	4	1.04	0.512
Residual	9			Residual	9		

744

745

746

747

748

749

750

751

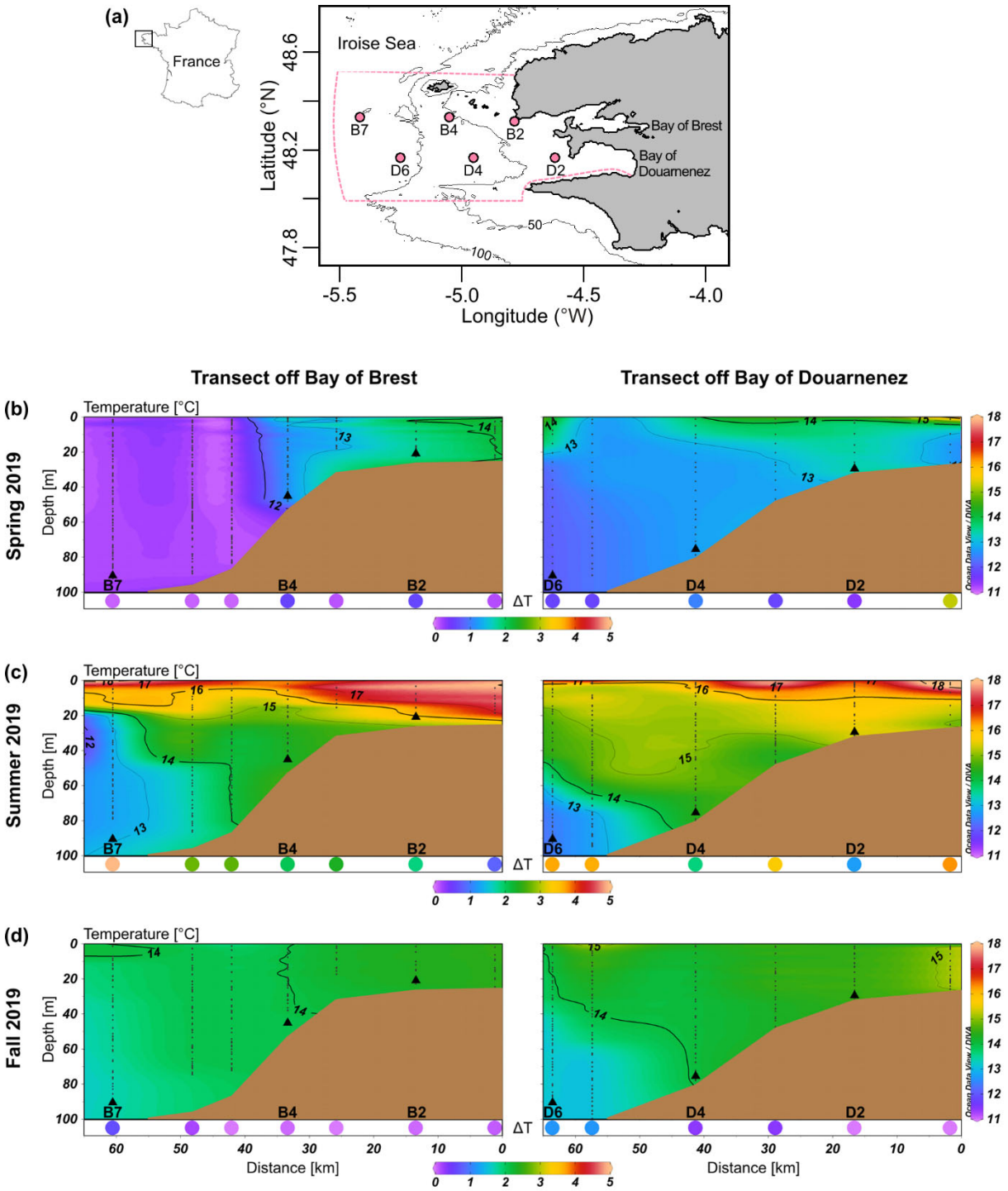

752

753 **Figure 1. Location of the study area and vertical profiles of temperature.** (a) Position of the
754 sampling stations in the Iroise Sea, along the transects off the bays of Brest (B2-B7) and
755 Douarnenez (D2-D6). The red dashed line represents the boundaries of the Iroise Marine Natural
756 Park. Vertical profiles of temperature, and stratification index (ΔT; indicated with color dots at the

bottom of the vertical temperature profiles) along the two transects during sampling in (b) spring, (c) summer, and (d) fall 2019. Triangles represent the starting depth of plankton tows. Vertical dashed lines indicate the location of CTD casts.

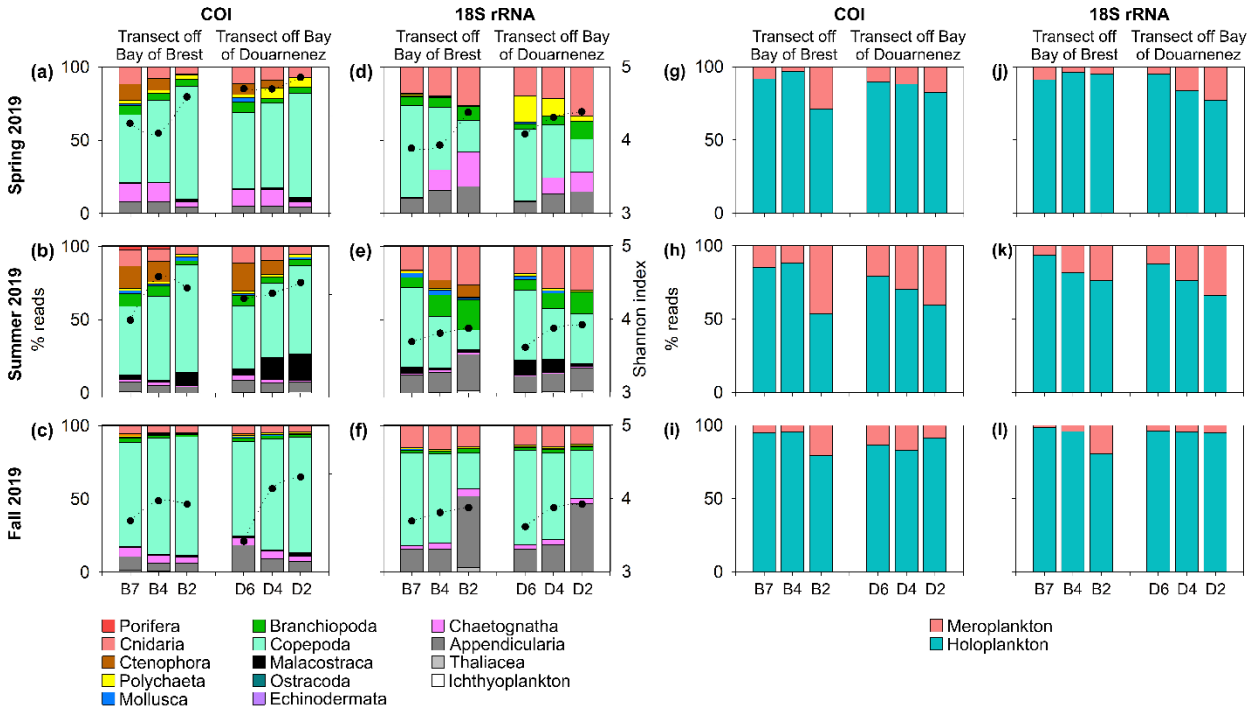

Figure 2. Proportion of reads of the mesozooplankton taxa, and reads associated to mero- and holoplankton. Proportion (percentage of reads) of mesozooplankton taxa with COI (a-c) and 18S (d-f) genes, and of mero- and holoplankton with COI (g-i) and 18S (j-l), in the Iroise Sea during spring, summer and fall 2019, along the two study transects. Black dots represent the Shannon diversity index. Taxa that represented less than 0.02% of the reads are not shown.

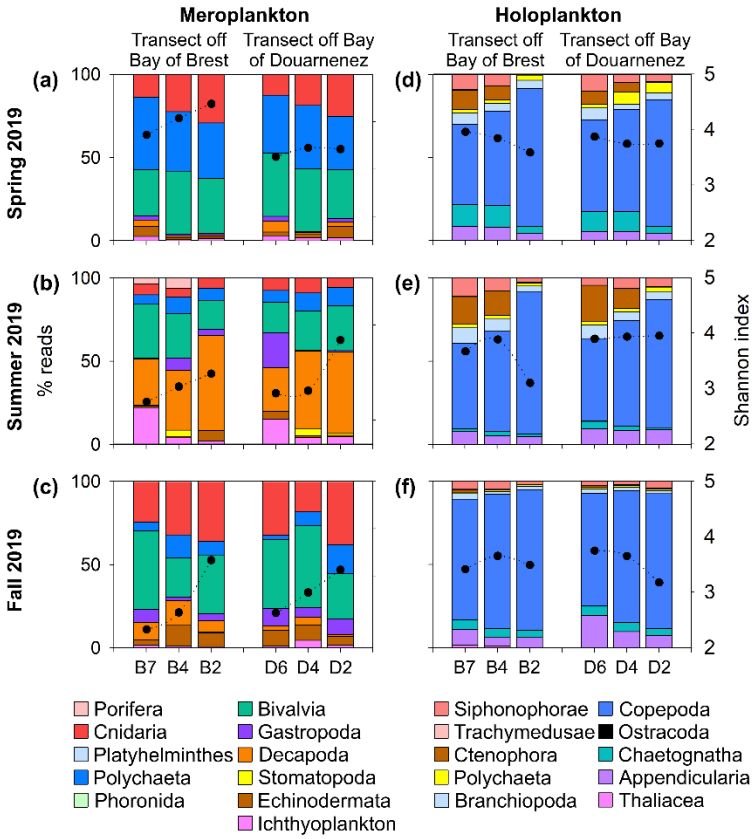

Figure 3. Proportion of main taxa for mero- and holoplankton. Proportion (percentage of reads) of the main taxa of mero- and ichthyoplankton (a-c) and holoplankton (d-f) in the Iroise Sea during spring, summer and fall 2019 with the COI gene. Black dots represent the Shannon diversity index.

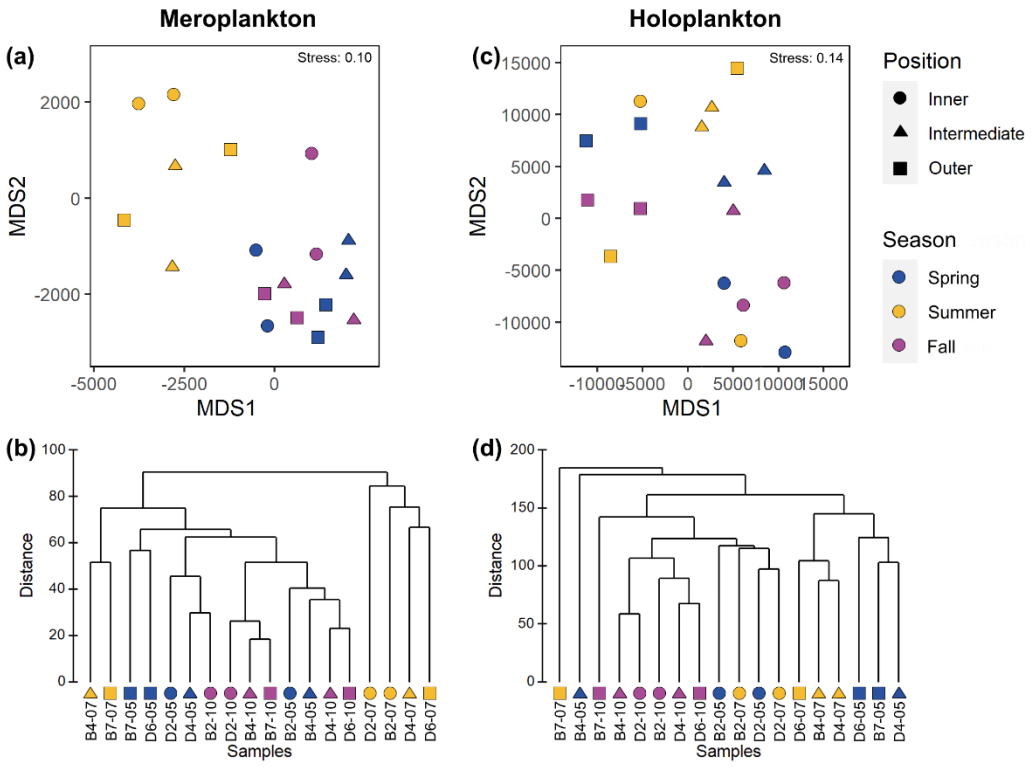

Figure 4. NMDS and clustering of the samples for mero- and holoplankton taxa. Nonmetric multidimensional scaling (nMDS) ordination and clustering of samples collected in the Iroise Sea based on the rarefied abundance (number of reads) of OTUs assigned to mero- (a,b) and holoplankton (c,d) taxa with the COI gene. Samples are classified according to shelf position and season of sampling.

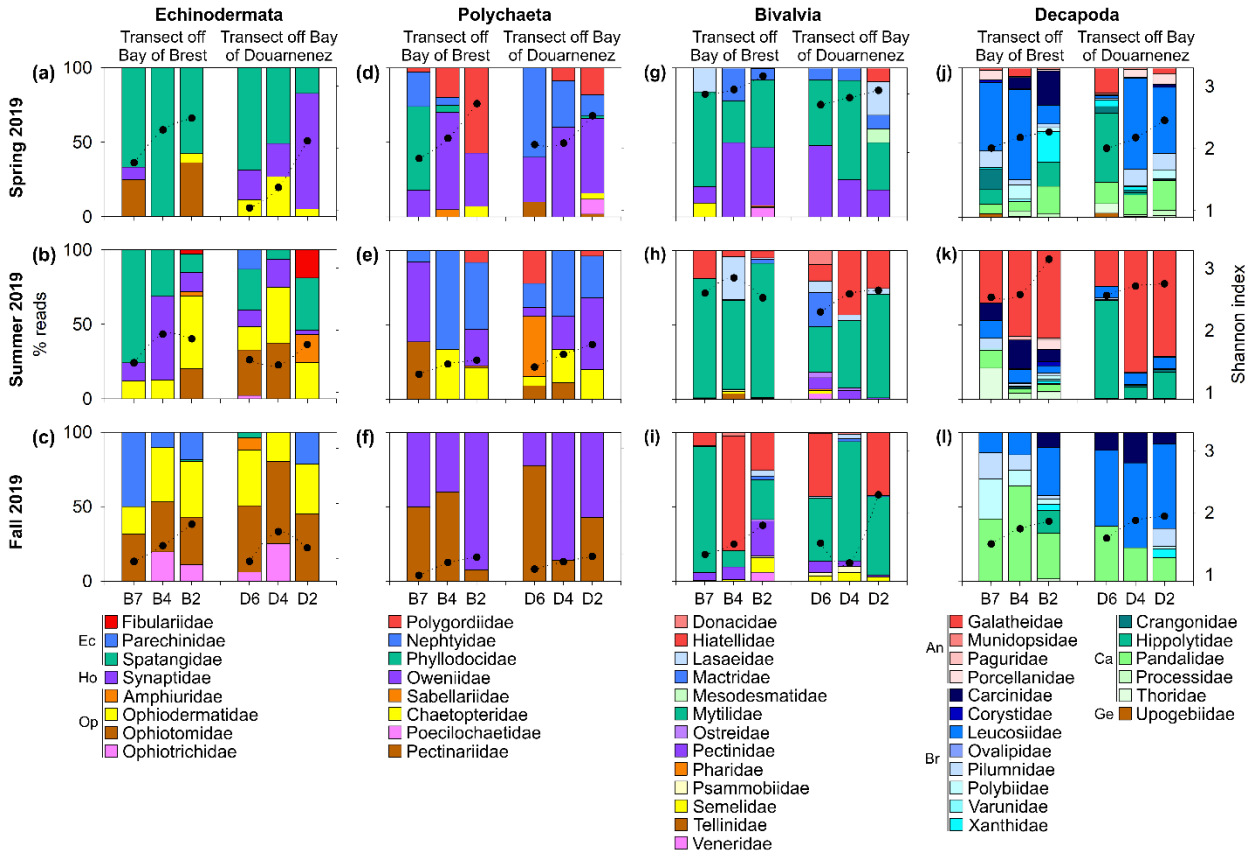

Figure 5. Community composition, at the family level, for Echinodermata, Polychaeta, Bivalvia and Decapoda, focusing on meroplankton. Proportion (percentage of reads) per family for Echinodermata (a-c), Polychaeta (d-f), Bivalvia (g-i) and Decapoda (j-l) in the Iroise Sea during spring, summer and fall 2019 with the COI gene. Black dots represent the Shannon diversity index. For echinoderms, Ec = Echinoidea, Ho = Holothuroidea, and Op = Ophiuroidea. For decapods, An = Anomura, Br = Brachyura, Ca = Caridea, and Ge = Gebiidea.

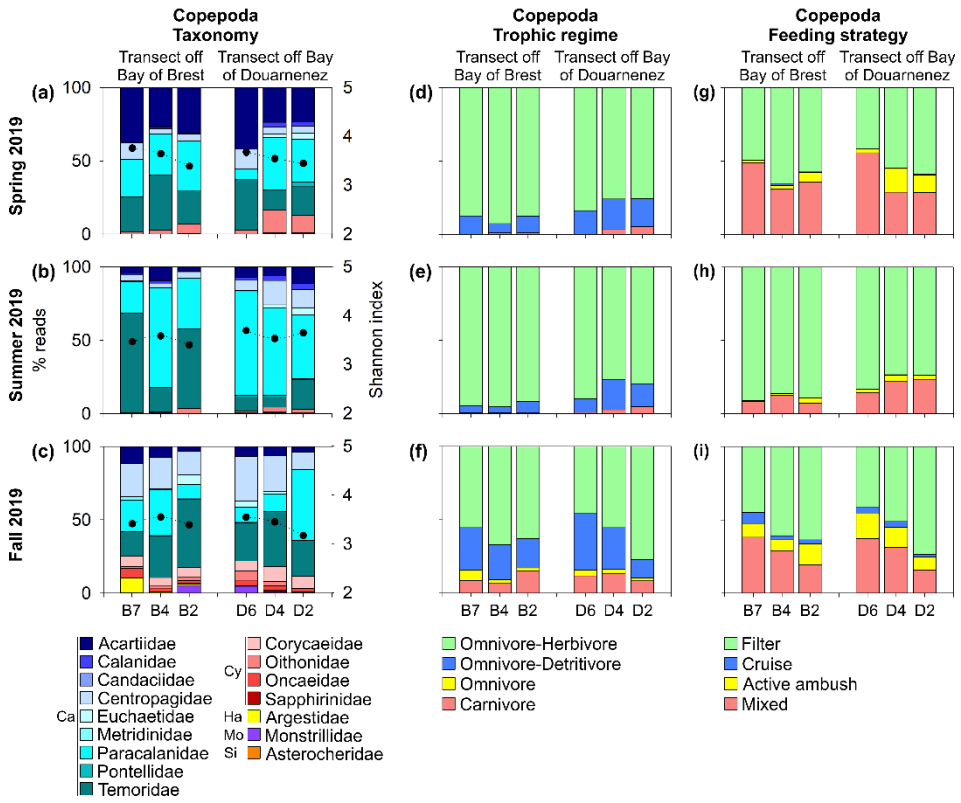

Figure 6. Taxonomic composition and feeding traits of copepods. Proportion (percentage of reads) of copepod families (a-c), and copepods feeding traits (d-i) in the Iroise Sea during spring, summer and fall 2019 as obtained from taxonomic assignment with the COI gene. Black dots represent the Shannon diversity index. Copepods are colored according to their Orders: Ca = Calanoida (shades of blue), Cy = Cyclopoida (shades of pink), Ha = Harpacticoida (yellow), Mo = Monstrilloida (purple), and Si = Siphonostomatoida (orange). Copepods traits based on available datasets (Benedetti *et al.*, 2015; Brun *et al.*, 2017).

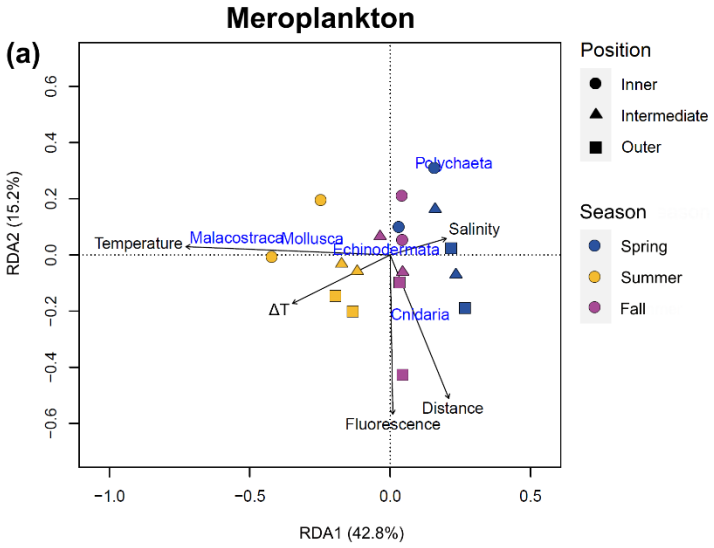
Meroplankton
(a)
Position
Inner
Intermediate
Outer
Season
Spring
Summer
Fall
Polychaeta
Salinity
Temperature
Malacostraca
Mollusca
Echinodermata
ΔT
Cnidaria
Distance
Fluorescence
RDA2 (15.2%)
RDA1 (42.8%)

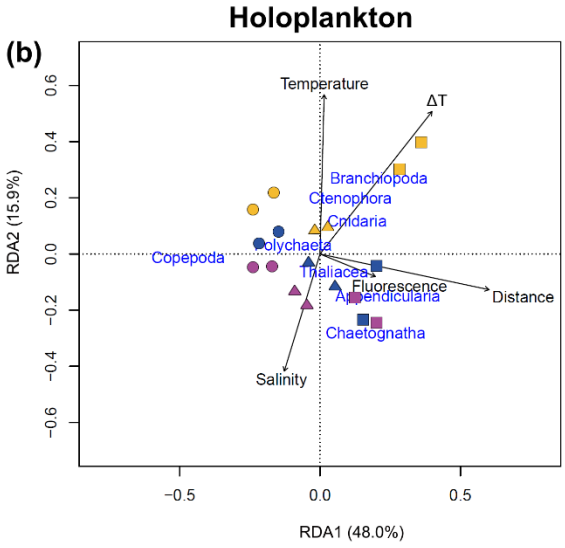
Holoplankton
(b)
Temperature
ΔT
Branchiopoda
Ctenophora
Cnidaria
Copepoda
Thaliacea
Fluorescence
Distance
Appendicularia
Chaetognatha
Salinity
RDA2 (15.9%)
RDA1 (48.0%)

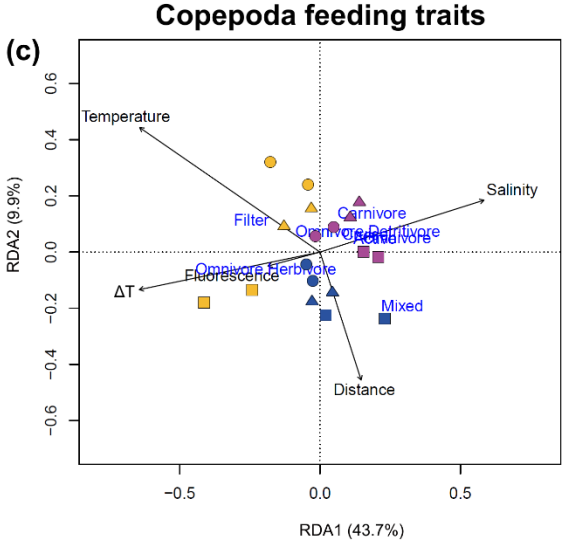
Copepoda feeding traits
(c)
Temperature
Salinity
Filter
Carnivore
Omnivore
Detritivore
Omnivore Herbivore
Fluorescence
ΔT
Mixed
Distance
RDA2 (9.9%)
RDA1 (43.7%)

Figure 7. Redundancy Analysis (RDA) ordination for meroplankton, holoplankton and copepods feeding traits in relation to environmental variables. Triplot of the RDA ordination with explanatory variables (arrows), taxa (abbreviations in blue) and samples (symbols), based on OTUs retrieved from the COI dataset and assigned to meroplankton (a), holoplankton (b), and copepods feeding traits (c). Samples are classified according to shelf position and season of sampling.